Electronic Supplementary Material (ESI) for New Journal of Chemistry.


# A compact prospective investigation on colorimetric recognition of $Hg^{2+}$ ion and photostimulated degradation of excreted toxic organic dyes motivated by *H. mutabilis* directed silver nanoparticles.

Somnath Das[a], Sharmistha Bera[a], Anukul Maji[a], SK Nayim[a], Gopal Ch. Jana[a], Maidul Hossain[a]*

[a] Department of Chemistry and Chemical Technology, Vidyasagar University, Midnapore-721102, West Bengal, India.

AUTHOR INFORMATION: Corresponding Author: Dr. Maidul Hossain, Department of Chemistry & Chemical Technology, Vidyasagar University, Midnapore-721102, West Bengal, India.*(M.H.) E-mail: hossainm@mail.vidyasagar.ac.in/ maidulhossain@yahoo.com

**Chemicals and reagents:**

In this whole research analytical standard chemicals were used Silver nitrate salt ($AgNO_3$, 99.99%), Toluidine Blue (TB), Rhodamine B (Rh-B) was imported from were purchased from renowned chemical company Sigma–Aldrich. *H. mutabilis* leaf was collected from Town colony, Medinipur, West Bengal, India. Used chemicals for cations sensing are in the form of water soluble common nitrate salt imported from Merck company (Darmstadt, Germany) which were $KNO_3$, $MgNO_3{\cdot}6H_2O$, $Ca(NO_3)_2{\cdot}4H_2O$, $Co(NO_3){\cdot}6H_2O$, $Mn(NO_3)_2{\cdot}4H_2O$, $Cd(NO_3)_2{\cdot}4H_2O$, $Cu(NO_3)_2{\cdot}3H_2O$, $Zn(NO_3)_2{\cdot}6H_2O$, $Pb(NO_3)_2$, $Hg(NO_3)_2{\cdot}H_2O$, $Cr(NO_3)_3\ {\cdot}9H_2O$, $Al(NO_3)_3.9H_2O$, $Fe(NO_3)_3.9H_2O$, $FeSO_4.7H_2O$, $Ni(NO_3)_2{\cdot}6H_2O$. All the involved apparatus were primarily washed out using aqua-regia followed by double distilled water and dried before use.

**Instruments used:**

All the photometric research was carried out by a computerized Shimadzu Pharmaspec 1601 unit model spectrophotometer (Shimadzu Corporation, Kyoto, Japan). Characterization of nanoparticles Hydrodynamic size and charge potential of the electrical layer (or zeta potential) were estimated on Malvern produced Zetasizer Nano instrument (Malvern, Worcestershire, UK). IR assessments of all the studied system were checked in liquid mode via a Perkin-Elmer Spectrum two FT-IR spectrophotometer attached with a diamond cell head sample analysis. X-Ray Diffraction (XRD) study was performed by Bruker D8 (Davinci System, Detector: Lynxeye (1D silicon strip technology, Target: Cu). Nanoparticles size/shape related justification was assessed by FESEM (Field Emission Electron Microscope, Carl Zeiss SMT AG, Germany) and HRTEM (High-Resolution Transmission Electron Microscope, JEM-2100, Tokyo, Japan). The elemental estimation was comprehended by EDX (Energy Dispersive X-ray) spectrometer. The average particle size histogram was visualized by Image J software (version 1.45S). X-ray Photoelectron Spectroscopy (XPS) measurement was performed through PHI 5000 Versa probe II Scanning XPS microprobe (excitation source: monochromatic Al Ka, ULVACPHI, USA). Gomori protocol was utilized for the preparation of standardized pH buffer solution measured by digital ORION VERSASTAR pH meter.

**Mechanism of HMNPs formation:**

The used plant extracted solution was itself playing dual character of stabilizing and reducing agent for nanoparticles formation. The biomolecules presented in every particular plant responsible for the reduction of silver ions and capping the reduced silver forming nanoparticles [1]. The extent of reducing or stabilizing property of that particular plant extract is solely its inherent property (depending on the phytochemical constituents ) thus the exact mechanism of plant mediated route based synthesis process of silver nanoparticles is obscure [2] [3]. However, here we provide a probable mechanism for nanoparticles formation depending on the experimental evidences Fig S1. It was pre researched that In H.mutabilis leaf extract (HME) flavonoids, protein and phenolic compounds were presented which play significant role in formation of nanoparticles [4]. From the FTIR spectra of HME it was revealed that The organic phytochemical constituent existing in the crude HME represented characteristic bands at 3620 $cm^{-1}$(-OH free), 3272 $cm^{-1}$ , 2932$cm^{-1}$(-OH stretch, carboxylic acid), 2712 $cm^{-1}$(-CH stretch, aldehyde),1660 $cm^{-1}$ (-CH stretch), 1543 $cm^{-1}$(C-C stretch, aromatic ring), 1170 $cm^{-1}$ (-CO stretch), 1063 $cm^{-1}$(-C-O-C stretch), 780 $cm^{-1}$(-CH out of plane bending, aromatic compounds).After formation of silver nanoparticles it was observed that almost all the bands of –OH and –CO were diminished. As a result, it can be summarized that the –OH, C=O, acid and C-O-C functional groups were the dominant stabilizing or reducing groups for stimulation of HMNPs synthesis. The same evidence obtained from XPS study which confirmed the –OH, C=O, acid and C-O-C group strongly capped the nanoparticles surface. As a whole during the formation of HMNPs first some of these groups were reduced the $Ag^{+}$ ion to $Ag^{0}$ than rest of the groups get capped at nanoparticles surface forming stable HMNPs solution. A probable mechanistic presentation was shown in Fig S1.

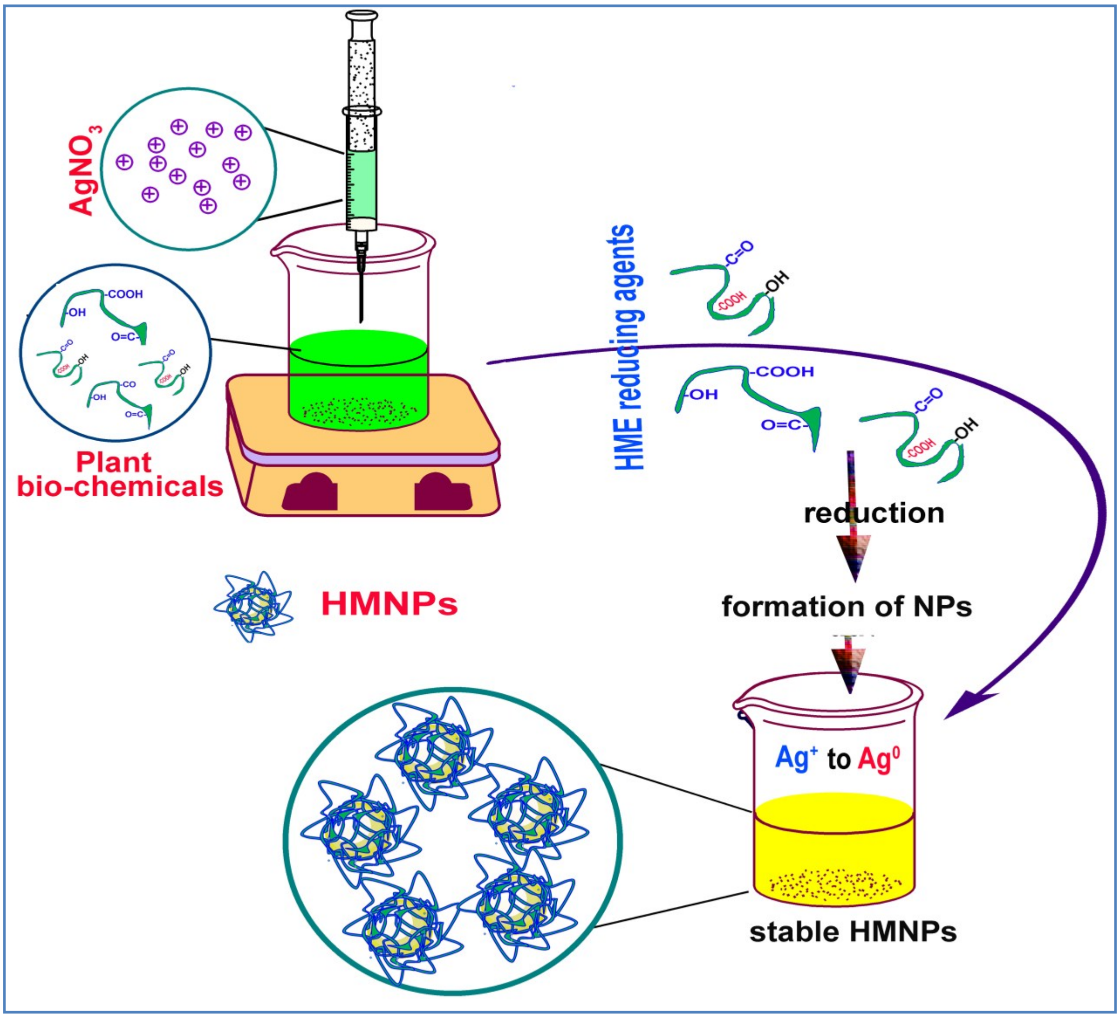


**Fig S1:** Probable mechanism of HMNPs formation with 3mM $Ag^{+}$ ion and HME.

**Concentration assessment of *HMNPs:***

Proper judgement of HMNPs concentration was assessed by UV–vis spectroscopy nominated molar extinction coefficient value 372396 × $10^3$ $M^{-1}$ $cm^{-1}$at wavelength 432 nm (depending on HRTEM directed size of HMNPs 8.36 nm) [1]. The working stock concentration of the HMNPs was finally estimated 1.86 × $10^{-9}$M.

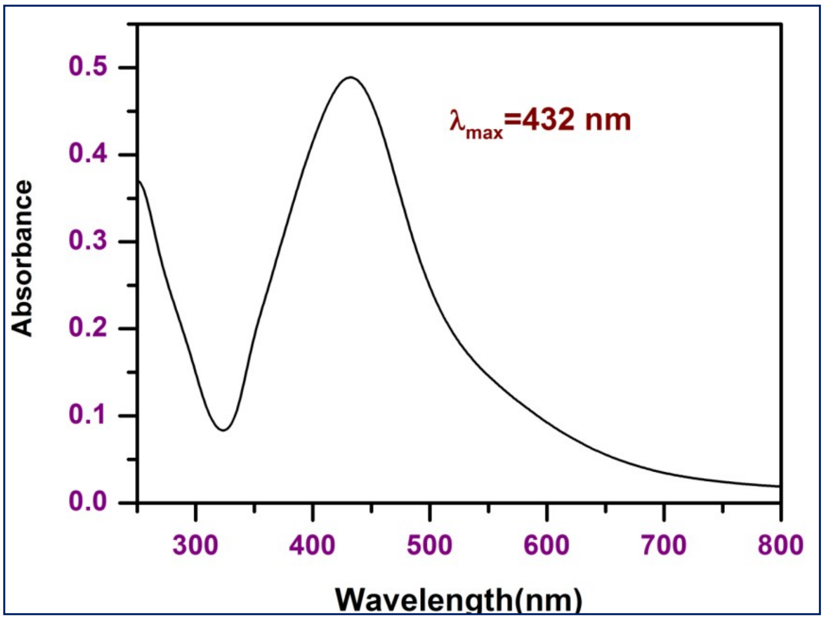


**Fig S2:** UV-vis spectra of pure HMNPs at 432 nm.

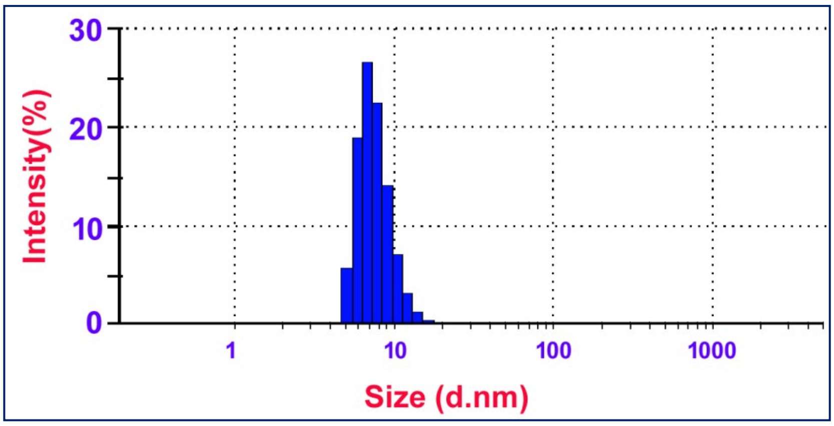


**Fig S3:** DLS image of pure HMNPs measured in water solution.

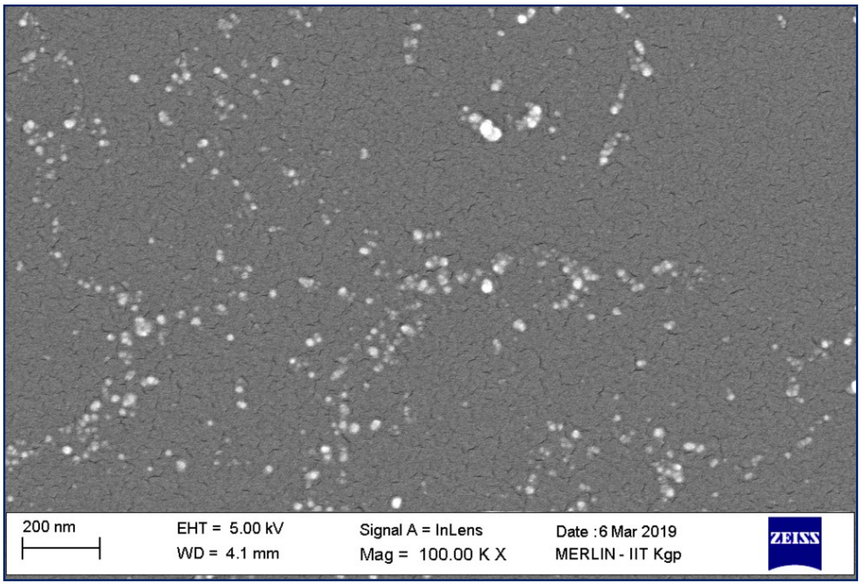


**Fig S4:** FESEM image of blank HMNPs dried on glass surface followed by vacuum drying.

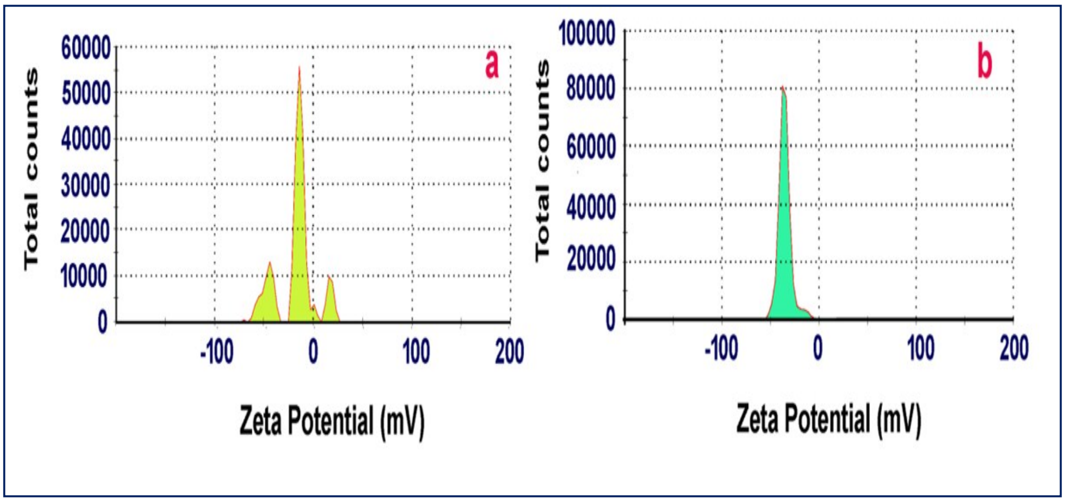


**Fig S5:** Zeta potential of (a) crude *H. mutabilis* leaf extract, (b) pure HMNPs.

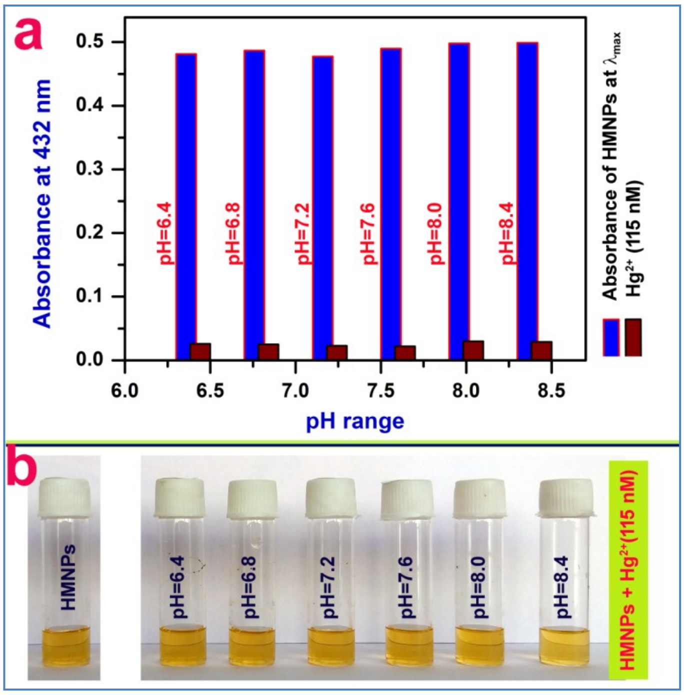


**Fig S6:** (a) Optimization of sensing response for $Hg^{2+}$ ion in a pH range 6.4 to 8.4 at 432 nm. (b) Evidence of no Photographic change of HMNPs at different pH.

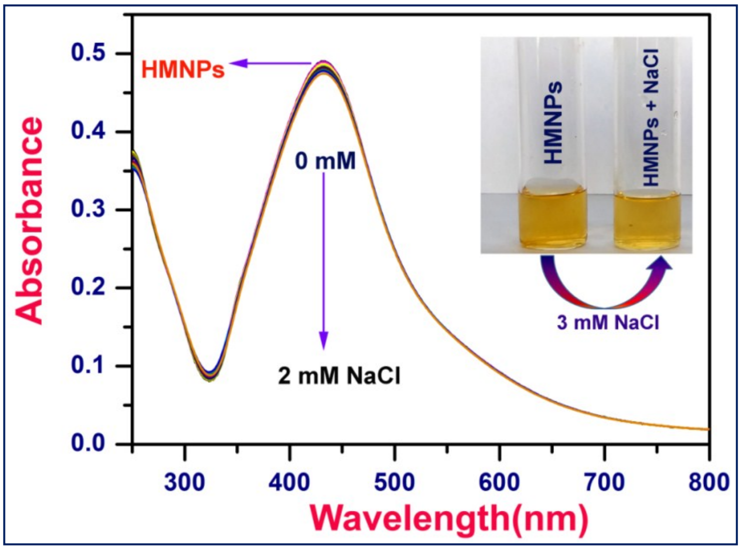


**Fig S7:** Represented the aggregation resistance potency of HMNPs at 3 mM NaCl conc.(Inset image was the photographic evidence of salt independent experiment).

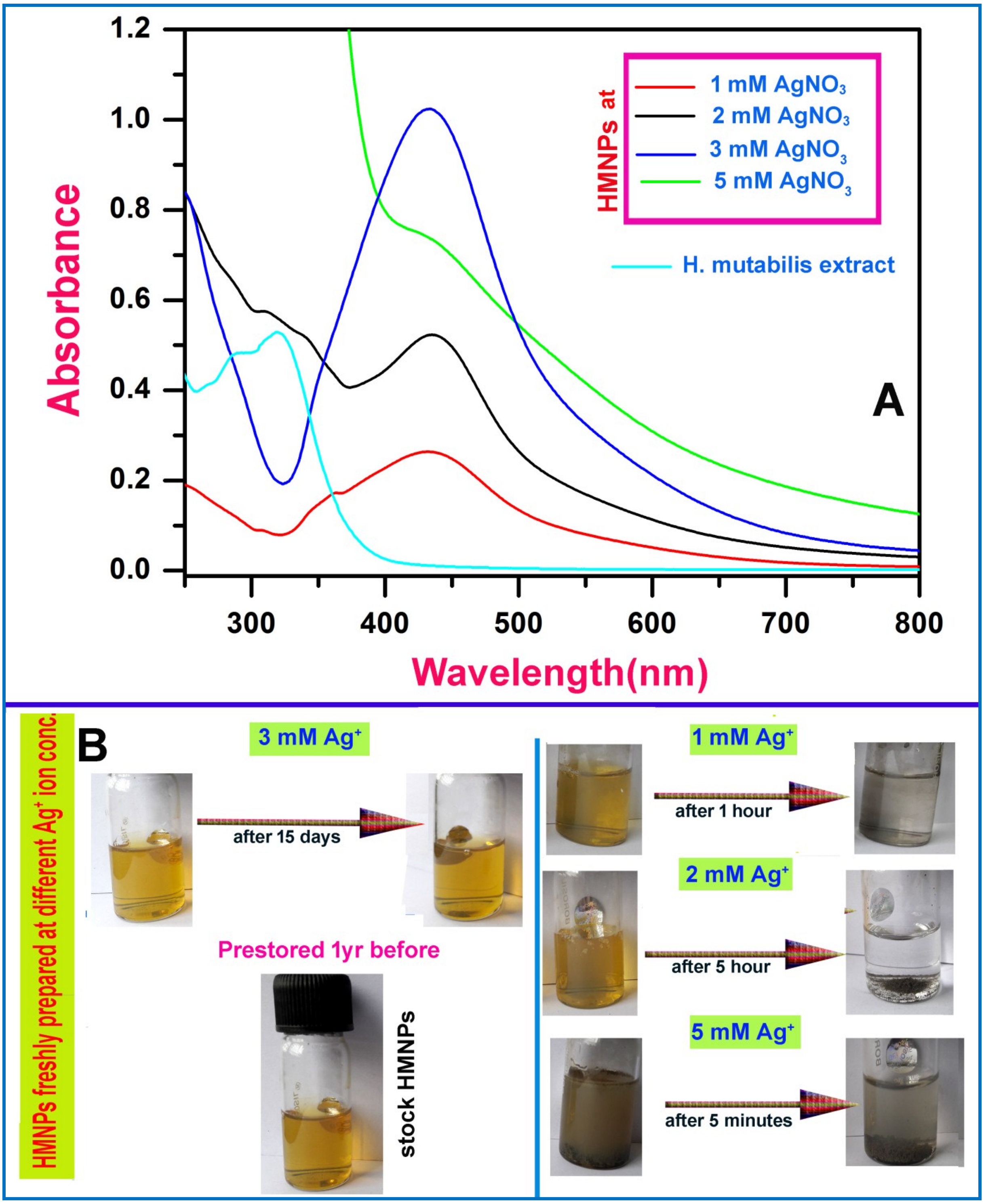


**Fig S8: (A)** UV-vis experiment for optimization of synthesis method for HMNPs y using variable Ag+ ion concentration (see inset). (B) Visual presentation of the all described HMNPs.

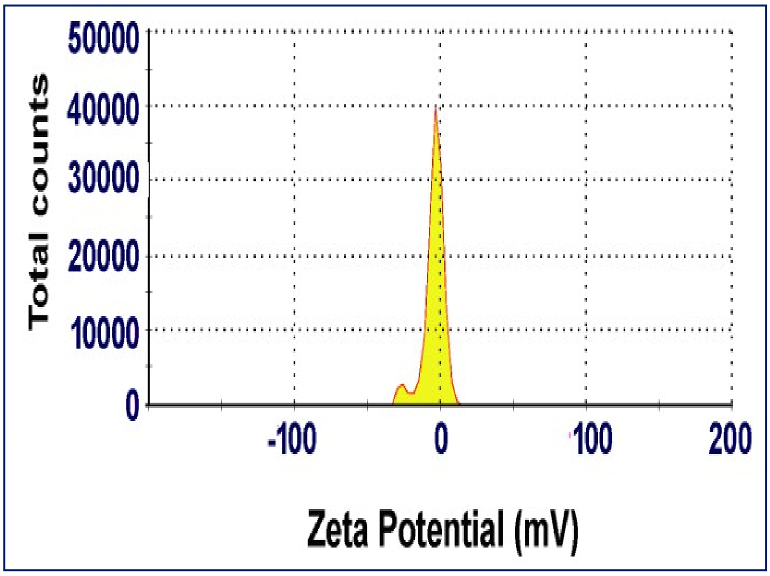


**Fig S9:** Zeta potential measurement of HMNPs in presence of 115 nM $Hg^{2+}$.

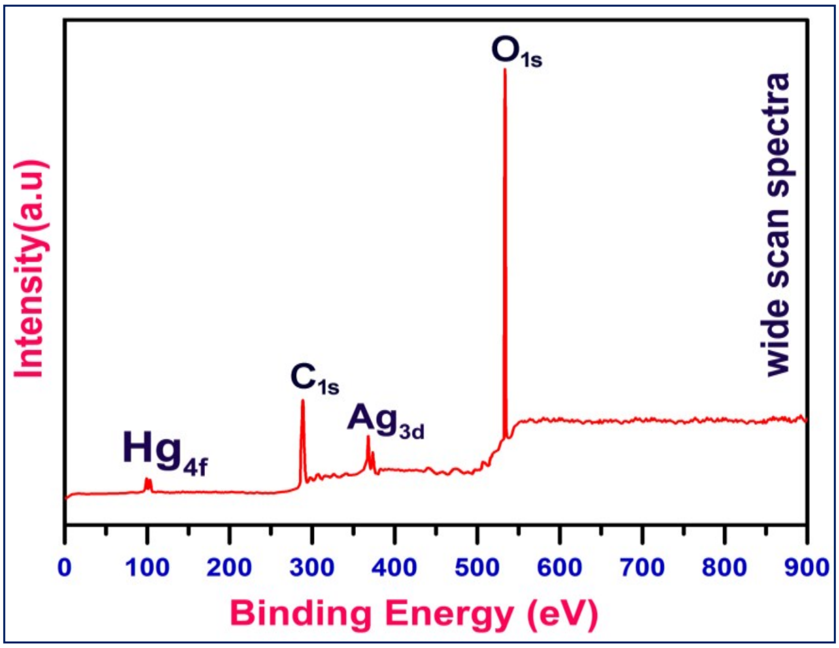


**Fig S10:** XPS wide scan survey of HMNPs in presence of $Hg^{2+}$.

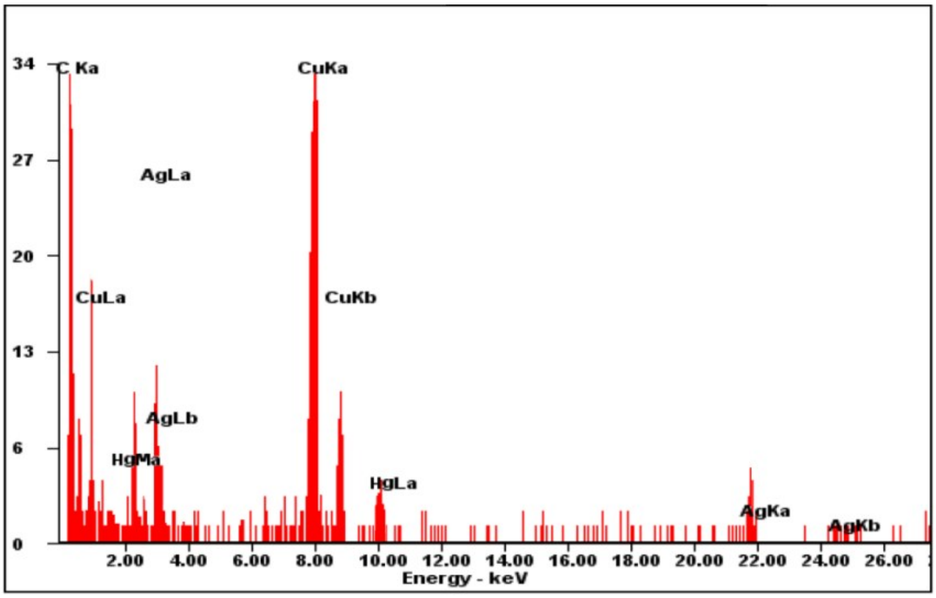


**Fig S11:** EDX elemental analysis of HMNPs in presence of 115 nM $Hg^{2+}$.

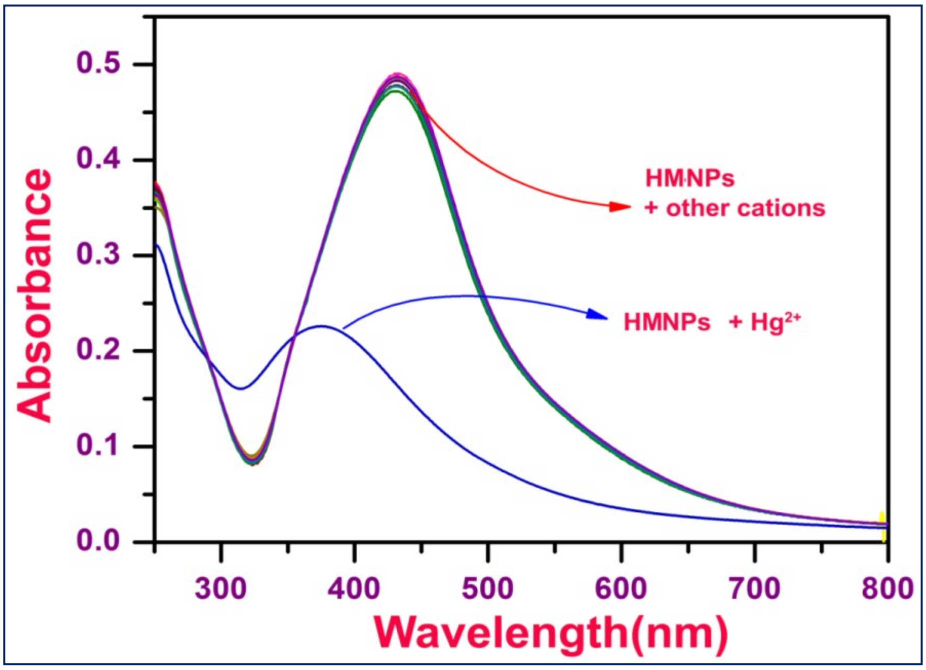


**Fig S12:** Competitive experiment for $Hg^{2+}$ ion selectivity assignment of HMNPs in presence of all other metal ion.

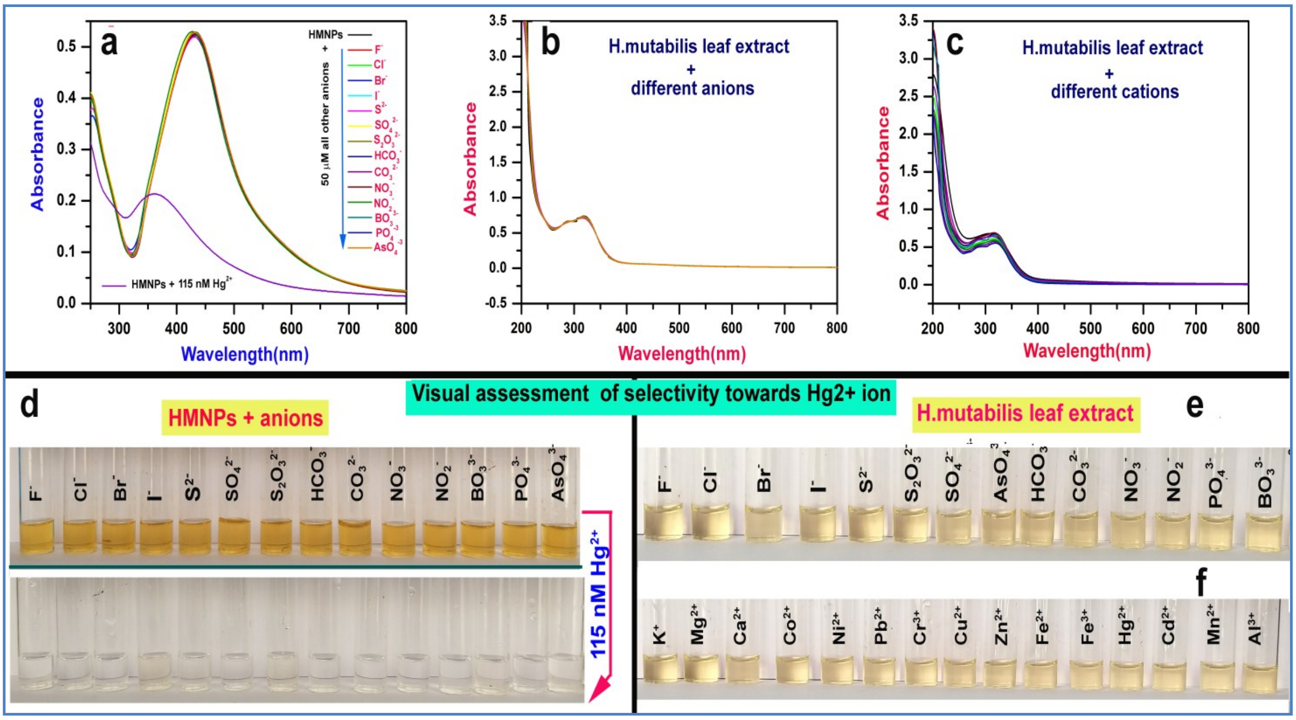


**Fig S13:** UV-visible and visual eye Selectivity assessment HMNPs (a, d) and response of the used *H. mutabilis* extract in presence of all ion (b, c, e & f).

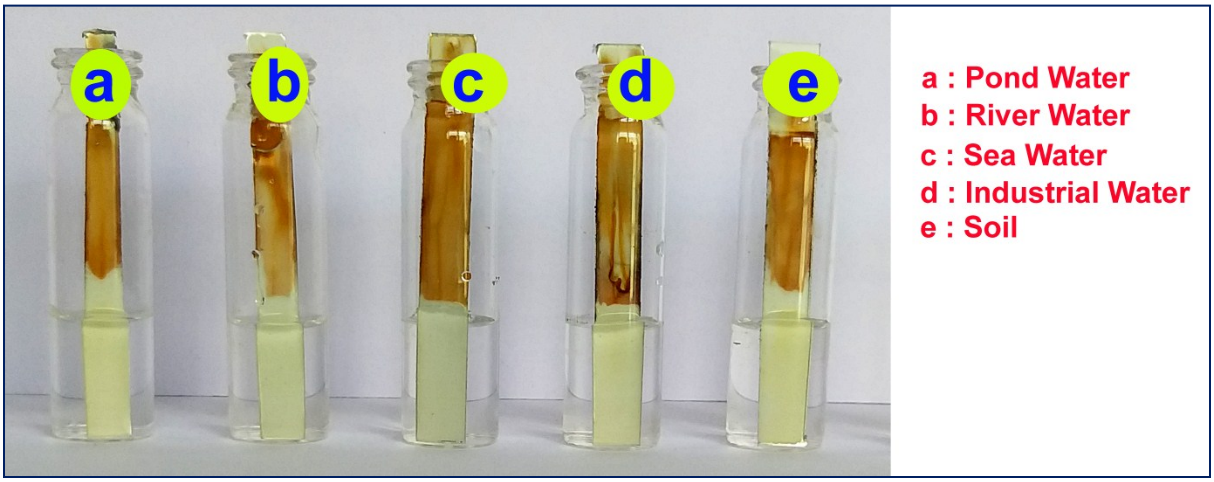


**Fig S14:** $Hg^{2+}$ ion sensing response of HMNPs strips on different real samples.

**Band Gap Calculation:**

It is essential to estimate either the nano particle have the potential of being an effective catalyst or not which can be only justified by evaluation of the optical band-gap energy ($E_g$). Stimulating, on this assignment we have calculated $E_g$ of HMNPs from the absorption spectra following the proposed $(\alpha hv)^2$ vs $(hv)$ plot using the equation from Tauc's theory appended below

$$(\alpha h\nu)=C\,(\alpha h\nu - E_g)^{1/n}$$

Thus, from the extra plotted portion of the linear part in Fig S12, $E_g$ was evaluated [2]. Here, α = the absorption coefficient (calculated according to $A = I/I_0 = e^{-ad}$ or from Beer–Lambert's relation, $\alpha = 2.303A/d$, where $d$ =path length (cm) of the quartz

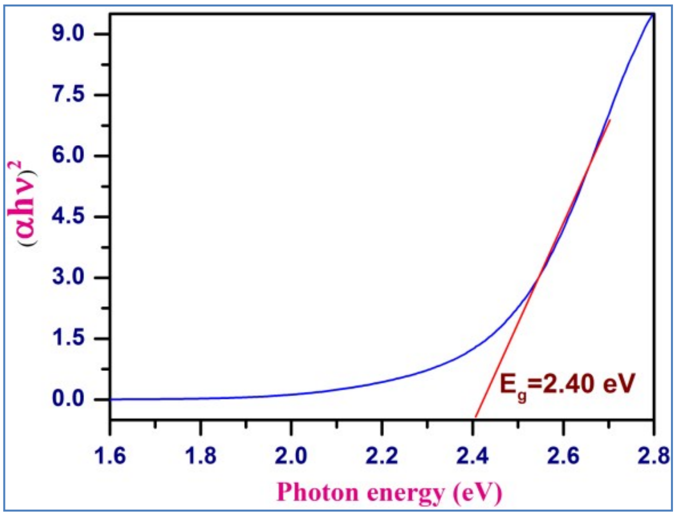


**Fig S15:** Band gap estimation of HMNPs

cuvette, A= absorbance of HMNPs) [3], $hv$= the photon energy, $E_g$=the direct band gap energy, C = constant, n=1/2 for direct approved transition for HMNPs[4]. The estimated optical band gap (Fig S15) of HMNPs was 2.40 eV.

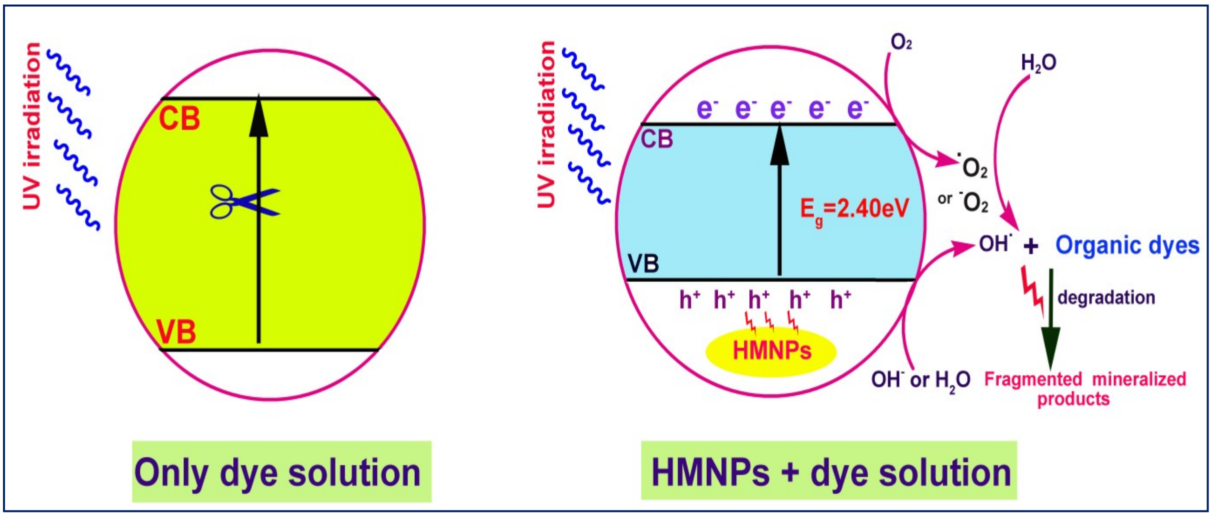


**Fig S16:** Schematic mechanistic evaluation of photo catalytic degradation stimulated by HMNPs.

**Preparation of strips for colorimetric detection of $Hg^{2+}$:**

In order to prepare the sensor strips we used cutting of TLC plates. We re-centrifuged the collected NPs and removing the upper clear solution. Then, we pipette out the suspended aliquots of NPs and deposit into the cutting of TLC plates. As soon as the TLC plates sock the aliquots and moved around the plate, we left the plates into desiccators (poured with solid $CaCl_2$ at bottom) for drying up to 1 hour. Now, they were taken out and collected for application.

**Collection and pretreatment of real samples for analysis:**

Real samples were collected from river( cossai river, midnapore, west bengal), sea water ( bay of bengal sea, orisa), Industrial water and soil (chemical waste drain and there around land from TATA chemicals). Before they are engaged into study we have performed a small pretreatment for them.

All **water samples** were boild up to 30 minutes and collected via filtration through a 0.22 mili micron filter paper( process is reperformed for another two times). These water samples were spiked with $Hg^{2+}$ at two different concentration and applied to the HMNPs.

For detection in soil, the collected **soil samples** were first dissolve in triple distilled water (1:5 gm/mL soil: water ratio) and the obtained solution were filtred by 0.22 mili micron filter paper( process is reperformed for another four times). Then, the collected water sample was spicked with $Hg^{2+}$ and applied to the poposed assay.

| **Table S1. $Hg^{2+}$detection methods published** | | | |
|---|---|---|---|
| Method | LOD | Ref. | Year |
| Lysine and dithiothreitol promoted ultrasensitive optical and colorimetric detection of mercury using anisotropic gold nanoparticles | $27\times10^{-3}$ nM & $58\times10^{-3}$nM | [5] | 2015 |
| Gold nanozyme-based paper chip for colorimetric detection of mercury ions | (30 μg L−1) | [6] | 2017 |
| Colorimetric Detection Of Mercury(II) Ion In Aqueous Solution Using Silver Nanoparticles | 850 nM | [7] | 2017 |
| Plasmonic detection of mercury via amalgam formation on surface-immobilized single Au nanorods | 45nM | [8] | 2017 |
| Dual mechanism-based sensing of mercury using unmodified ,heteroepitaxially synthesized silver nanoparticles | 100 nM | [9] | 2017 |

| | | | |
|---|---|---|---|
| Sensitive and robust colorimetric assay of Hg2+ and S2− in aqueous solution directed by 5-sulfosalicylic acid-stabilized silver nanoparticles for wide range application in real samples | 14 nM | [10] | 2017 |
| Label-Free Colorimetric Detection of Mercury (II) Ions Based on Gold Nanocatalysis | 10 nM | [11] | 2018 |
| Colorimetric sensing of mercury (II) ion based on anti aggregation of gold nanoparticles in the presence of hexadecyl trimethyl ammonium bromide | 11.9nM | [12] | 2018 |
| A Highly Sensitive and Selective Colorimetric $Hg^{2+}$ Ion Probe Using Gold Nanoparticles Functionalized with Polyethyleneimine | 1.72 nM | [13] | 2018 |
| Thiol terminated chitosan capped silver nanoparticles for sensitive and selective detection of mercury (II) ions in water | 5ppb | [14] | 2018 |
| Colorimetric and visual detection of mercury(II) based on the suppression of the interaction of dithiothreitol with agar-stabilized silver-coated gold nanoparticles | 78 nM | [15] | 2018 |
| Mercaptobenzoheterocyclic compounds functionalized silver nanoparticle, an ultrasensitive colorimetric probe for Hg(II) detection in water with picomolar precision: A correlation between | 46, 92 pM | [16] | 2018 |

| | | | |
|---|---|---|---|
| sensitivity and binding affinity | | | |
| Colorimetric Detection of Mercury Ions in Water with Capped Silver Nanoprisms | $1.5\times10^3$ nM | [17] | 2019 |
| Paper-based electrochemical transducer modified with nanomaterials for mercury determination in environmental waters | 30nM | [18] | 2019 |
| Ratiometric detection of heavy metal ions using fluorescent carbon dots | 37.5 nM | [19] | 2019 |
| Green and simple synthesis route of Ag@AgCl nanomaterial using green marine crude extract and its application for sensitive and selectivedetermination of mercury | 4.19 nM | [20] | 2019 |
| Chromogenic vesicles for aqueous detection and quantification of $Hg^{2+}/Cu^{2+}$ in real water samples | 30 nM | [21] | 2019 |
| Covalent Organic Framework Nanosheet-Based Ultrasensitive and Selective Colorimetric Sensor for Trace $Hg^{2+}$ Detection | 0.33nM | [22] | 2019 |
| Optimization of Plasmonic U-Shaped Optical Fiber Sensor for Mercury Ions Detection Using Glucose Capped Silver Nanoparticles | 2ppb & 5ppb | [23] | 2019 |
| Catalytic Degradation of Methyl Orange and Selective Sensing of Mercury Ion in Aqueous Solutions Using Green Synthesized Silver Nanoparticles from the Seeds of *Derris trifoliata* | $1.55\times10^3$ nM | [24] | 2019 |

| | | | |
|---|---|---|---|
| | | | |
| Phytosynthesis of silver nanoparticles; naked eye cellulose filter paper dual mechanism sensor for mercury ions and ammonia in aqueous solution | 5ppb | [25] | 2019 |
| A reversible biocompatible silver nanoconstracts for selective sensing of mercury ions combined with antimicrobial activity studies | 830 nM | [26] | 2019 |
| Colorimetric determination of mercury(II) using gold nanoparticles and double ligand exchange | 24 nM | [27] | 2019 |
| A sensorial colorimetric detection method for $Hg^{2+}$ and $Cu^{2+}$ ions using single probe sensor based on 5-methyl-1,3,4-thiadiazole-2-thiol stabilized gold nanoparticles and its application in real water sample analysis | 14 nM | [28] | 2019 |
| Colorimetric and naked eye detection of trace Hg2+ ions in the environmental water samples based on plasmonic response of sodium alginate impregnated by silver nanoparticles | 5.29 nM | [29] | 2019 |
| Construction of an effective ratiometric fluorescent sensing platform for specific and visual detection of mercury ions based on target-triggered the | 38 pM | [30] | 2019 |

| | | | |
|---|---|---|---|
| inhibition on inner filter effect | | | |
| Determination of $Hg^{2+}$ and $Cu^{2+}$ ions by dual-emissive Ag/Au nanocluster/ carbon dots nanohybrids: Switching the selectivity by pH adjustment | 7 nM | [31] | 2019 |
| Synthesis of Calixarene-Capped Silver Nanoparticles for Colorimetric and Amperometric Detection of Mercury (HgII, Hg0) | 0.5 nM | [32] | 2019 |
| Our studied method | **~ 48 pM** | | |

**Reference:**


[1] S. Das, A. Das, A. Maji, M. Beg, A. Singha, M. Hossain, A compact study on impact of multiplicative Streblus asper inspired biogenic silver nanoparticles as effective photocatalyst, good antibacterial agent and interplay upon interaction with human serum albumin, Journal of Molecular Liquids, 259 (2018) 18-29.

[2] D.S. Seigler, Diterpenes and Sesterterpenes, in: Plant Secondary Metabolism, Springer US, Boston, MA, 1998, pp. 398-426.

[3] J.G. Luis, Chemistry, biogenesis, and chemotaxonomy of the diterpenoids of Salvia. In: Harborne, in: T.-B. J.B., F.A. (Ed.) Ecological Chemistry and Biochemistry of Plant Terpenoids, Clarendon Press, Oxford 1991.

[4] Z. Hou, X. Liang, F. Su, W. Su, Preparative isolation and purification of seven compounds from Hibiscus mutabilis L. leaves by two-step high-speed counter-current chromatography, Chemical Industry and Chemical Engineering Quarterly, 21 (2015) 331-341.

[5] A. Chaudhary, C. Dwivedi, M. Chawla, A. Gupta, C.K. Nandi, Lysine and dithiothreitol promoted ultrasensitive optical and colorimetric detection of mercury using anisotropic gold nanoparticles, Journal of Materials Chemistry C, 3 (2015) 6962-6965.

[6] K.N. Han, J.-S. Choi, J. Kwon, Gold nanozyme-based paper chip for colorimetric detection of mercury ions, Scientific Reports, 7 (2017) 2806.

[7] M.L. Firdaus, I. Fitriani, S. Wtantuti, Y.W. Hartati, R. Khaydarov, J.A. Mcalister, H. Obata, T. Gamo, Colorimetric Detection of Mercury(II) Ion in Aqueous Solution Using Silver Nanoparticles

Analytical Sciences, 33 (2017) 831-837.

[8] C. Schopf, A. Martín, D. Iacopino, Plasmonic detection of mercury via amalgam formation on surface-immobilized single Au nanorods, Science and Technology of Advanced Materials, 18 (2017) 60-67.

[9] A. Nain, S.R. Barman, S. Jain, A. Mukherjee, J. Satija, Dual mechanism-based sensing of mercury using unmodified, heteroepitaxially synthesized silver nanoparticles, Applied Nanoscience, 7 (2017) 299-307.

[10] S. Das, M.N. Aktara, N.K. Sahoo, P.K. Jha, M. Hossain, Sensitive and robust colorimetric assay of Hg2+ and S2− in aqueous solution directed by 5-sulfosalicylic acid-stabilized silver nanoparticles for wide range application in real samples, Journal of Environmental Chemical Engineering, 5 (2017) 5645-5654.

[11] P.W. Yang, T.; Lin, Y., Label-Free Colorimetric Detection of Mercury (II) Ions Based on Gold Nanocatalysis. , Sensors, 18 (2018) 2807.

[12] X. Sun, R. Liu, Q. Liu, Q. Fei, G. Feng, H. Shan, Y. Huan, Colorimetric sensing of mercury (II) ion based on anti-aggregation of gold nanoparticles in the presence of hexadecyl trimethyl ammonium bromide, Sensors and Actuators B: Chemical, 260 (2018) 998-1003.

[13] K.M. Kim, Y.-S. Nam, Y. Lee, K.-B. Lee, A Highly Sensitive and Selective Colorimetric Hg2+ Ion Probe Using Gold Nanoparticles Functionalized with Polyethyleneimine, Journal of Analytical Methods in Chemistry, 2018 (2018) 12.

[14] P. Sharma, M. Mourya, D. Choudhary, M. Goswami, I. Kundu, M.P. Dobhal, C.S.P. Tripathi, D. Guin, Thiol terminated chitosan capped silver nanoparticles for sensitive and selective detection of mercury (II) ions in water, Sensors and Actuators B: Chemical, 268 (2018) 310-318.

[15] Q. Da, Y. Gu, X. Peng, L. Zhang, S. Du, Colorimetric and visual detection of mercury(II) based on the suppression of the interaction of dithiothreitol with agar-stabilized silver-coated gold nanoparticles, Microchimica Acta, 185 (2018) 357.

[16] Y. Bhattacharjee, D. Chatterjee, A. Chakraborty, Mercaptobenzoheterocyclic compounds functionalized silver nanoparticle, an ultrasensitive colorimetric probe for Hg(II) detection in water with picomolar precision: A correlation between sensitivity and binding affinity, Sensors and Actuators B: Chemical, 255 (2018) 210-216.

[17] F. Tanvir, A. Yaqub, S. Tanvir, R. An, W.A. Anderson, Colorimetric Detection of Mercury Ions in Water with Capped Silver Nanoprisms. , Materials 12 (2019) 1533.

[18] A. Sánchez-Calvo, M.T. Fernández-Abedul, M.C. Blanco-López, A. Costa-García, Paper-based electrochemical transducer modified with nanomaterials for mercury determination in environmental waters, Sensors and Actuators B: Chemical, 290 (2019) 87-92.

[19] F. Yarur, J.-R. Macairan, R. Naccache, Ratiometric detection of heavy metal ions using fluorescent carbon dots, Environmental Science: Nano, 6 (2019) 1121-1130.

[20] S. Karimi, T. Samimi, Green and simple synthesis route of Ag@AgCl nanomaterial using green marine crude extract and its application for sensitive and selective determination

of mercury, Spectrochimica Acta Part A: Molecular and Biomolecular Spectroscopy, 222 (2019) 117216.

[21] T. Rasheed, F. Nabeel, S. Shafi, Chromogenic vesicles for aqueous detection and quantification of Hg2+/Cu2+ in real water samples, Journal of Molecular Liquids, 282 (2019) 489-498.

[22] W.-R. Cui, C.-R. Zhang, W. Jiang, R.-P. Liang, S.-H. Wen, D. Peng, J.-D. Qiu, Covalent Organic Framework Nanosheet-Based Ultrasensitive and Selective Colorimetric Sensor for Trace Hg2+ Detection, ACS Sustainable Chemistry & Engineering, 7 (2019) 9408-9415.

[23] G. Shukla, N. Punjabi, T. Kundu, S. Mukherji, Optimization of Plasmonic U-Shaped Optical Fiber Sensor for Mercury Ions Detection Using Glucose Capped Silver Nanoparticles, 2019.

[24] N. Cyril, J.B. George, L. Joseph, V.P. Sylas, Catalytic Degradation of Methyl Orange and Selective Sensing of Mercury Ion in Aqueous Solutions Using Green Synthesized Silver Nanoparticles from the Seeds of Derris trifoliata, Journal of Cluster Science, 30 (2019) 459-468.

[25] M. Ismail, M.I. Khan, K. Akhtar, J. Seo, M.A. Khan, A.M. Asiri, S.B. Khan, Phytosynthesis of silver nanoparticles; naked eye cellulose filter paper dual mechanism sensor for mercury ions and ammonia in aqueous solution, Journal of Materials Science: Materials in Electronics, 30 (2019) 7367-7383.

[26] I. Sk, M.A. Khan, S. Ghosh, D. Roy, S. Pal, S. Homechuadhuri, M.A. Alam, A reversible biocompatible silver nanoconstracts for selective sensing of mercury ions combined with antimicrobial activity studies, Nano-Structures & Nano-Objects, 17 (2019) 185-193.

[27] D. Huang, X. Liu, C. Lai, L. Qin, C. Zhang, H. Yi, G. Zeng, B. Li, R. Deng, S. Liu, Y. Zhang, Colorimetric determination of mercury(II) using gold nanoparticles and double ligand exchange, Microchimica Acta, 186 (2018) 31.

[28] M.N. Aktara, S. Das, S. Nayim, N.K. Sahoo, M. Beg, G.C. Jana, A. Maji, P.K. Jha, M. Hossain, A sensorial colorimetric detection method for Hg2+ and Cu2+ ions using single probe sensor based on 5-methyl-1,3,4-thiadiazole-2-thiol stabilized gold nanoparticles and its application in real water sample analysis, Microchemical Journal, 147 (2019) 1163-1172.

[29] F. Faghiri, F. Ghorbani, Colorimetric and naked eye detection of trace Hg2+ ions in the environmental water samples based on plasmonic response of sodium alginate impregnated by silver nanoparticles, Journal of Hazardous Materials, 374 (2019) 329-340.

[30] L. Han, S.G. Liu, X.Z. Dong, J.Y. Liang, N.B. Li, H.Q. Luo, Construction of an effective ratiometric fluorescent sensing platform for specific and visual detection of mercury ions based on target-triggered the inhibition on inner filter effect, Journal of Hazardous Materials, 376 (2019) 170-177.

[31] E. Babaee, A. Barati, M.B. Gholivand, A. Taherpour, N. Zolfaghar, M. Shamsipur, Determination of Hg2+ and Cu2+ ions by dual-emissive Ag/Au nanocluster/carbon dots nanohybrids: Switching the selectivity by pH adjustment, Journal of Hazardous Materials, 367 (2019) 437-446.

[32] G. Vyas, S. Bhatt, P. Paul, Synthesis of Calixarene-Capped Silver Nanoparticles for Colorimetric and Amperometric Detection of Mercury (HgII, Hg0), ACS Omega, 4 (2019) 3860-3870.